EXPERIMENTAL AND ANALYTICAL INVESTIGATION OF THE MTS WATER-COOLED TARGET THERMAL-HYDRAULIC CHARACTERISTICS

Curtt Ammerman and Keith Woloshun

Los Alamos National Laboratory, Los Alamos, New Mexico, 87545, ammerman@lanl.gov

The Material Test Station (MTS) will provide a domestic, fast-spectrum, neutron irradiation facility located at Los Alamos National Laboratory. The facility will provide proof-of-performance test capabilities for AFCI and GEN IV fuels and materials. The MTS will use the LANSCE accelerator pulsed proton beam (800 MeV, 1.25 mA) to illuminate two target sections creating a flux trap where fuel and material samples can be irradiated. The target sections consist of a series of tungsten plates with narrow, 1-mm-wide coolant channels between them. A requirement of the facility is to create a neutron flux similar to that of a fast reactor with a peak fast neutron flux of at least 10^{15} n/cm^2/s. To achieve the necessary flux, a high beam current density on target is required. This current density results in a peak target plate heat flux of 6 MW/m^2. This paper presents the results of experimental and analytical investigations of the thermal-hydraulic characteristics of a water-cooled target design. These results include single-phase heat transfer coefficient, channel pressure drop, and onset of nucleate boiling.

I. INTRODUCTION

The Material Test Station (MTS) is a proposed domestic, fast-spectrum, neutron irradiation facility. The facility will provide proof-of-performance test capabilities for AFCI and GEN IV fuels and materials. The MTS will be built in Area A of the Los Alamos Neutron Science Center (LANSCE) at Los Alamos National Laboratory. The facility will use the LANSCE accelerator pulsed proton beam (800 MeV, 1.25 mA) to illuminate two target sections creating a flux trap where fuel and material samples can be irradiated. Figure 1 shows the MTS target concept. A requirement of the facility is to create a neutron flux similar to that of a fast reactor with a peak fast flux of at least 10^{15} n/cm^2/s. To achieve the necessary flux, a high beam current density of 75 μA/cm^2 on target is required. This high current density results in a peak target plate heat flux of 6 MW/m^2. Two different coolants are currently being considered for the MTS target: single-phase, heavy water (D_2O), and lead-bismuth eutectic (LBE). This paper addresses the water-cooled design.

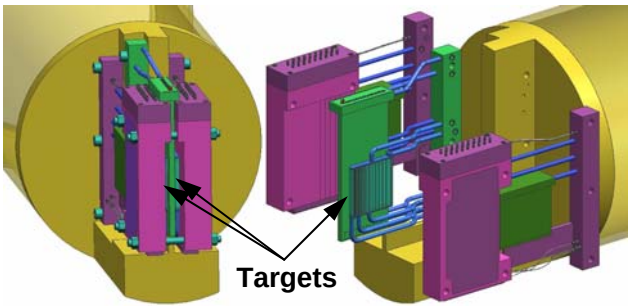

Fig. 1. MTS target concept (exploded view on right).

The target sections, shown in Fig. 2, are a series of closely spaced tungsten plates with progressive thicknesses (4.4-12 mm) according to energy deposition rates. Plate thickness is limited to maintain surface heat flux at or below 6 MW/m^2. The plates (Fig. 3) consist of a tungsten core clad with tantalum to prevent water corrosion. This design is based on proven technology developed for ISIS[1] and KENS[2]. Each target half is cooled by series flow of water in five parallel paths. Water flows between target plates in narrow channels to minimize water volume and provide high heat transfer coefficients. The channel dimension is 1 mm high x 18 mm wide x 180 mm long. The beam spot on target is a rectangle that is 15 mm wide by 60 mm high. The normalized beam spot intensity is shown in Fig. 4 over the 15 mm nominal spot width.

The target was designed to operate with single-phase heat transfer to avoid flow instabilities caused by boiling. The pressure in the target was elevated to suppress boiling. The design coolant inlet and outlet conditions for 5 channels in series are shown in Table 1. The heat transfer coefficient of 54,000 W/m^2°C was obtained for the first channel using the correlation of Sieder and Tate[3] and conservatively reducing it by 20%. Combining this heat transfer coefficient with the coolant outlet temperature results in a predicted outlet wall temperature of 225°C. The pressure drop for the channels was estimated assuming turbulent flow with a smooth-wall Moody friction factor. The outlet conditions result in a subcooling level of 101°C.

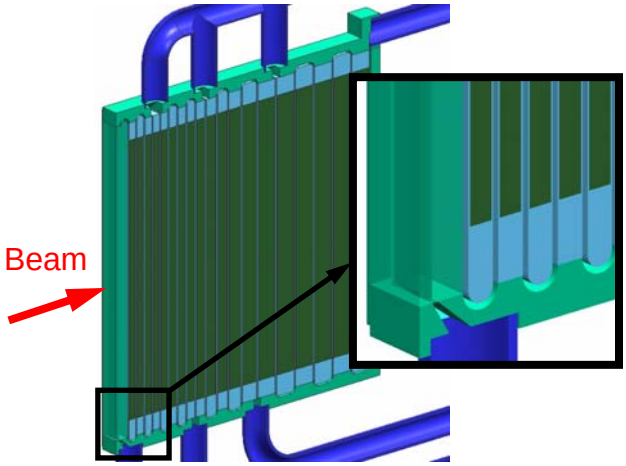

Fig. 2. Section view of target showing target plates and cooling channels.

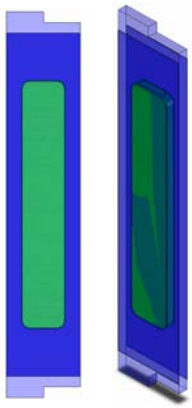

Fig. 3. Target plates.

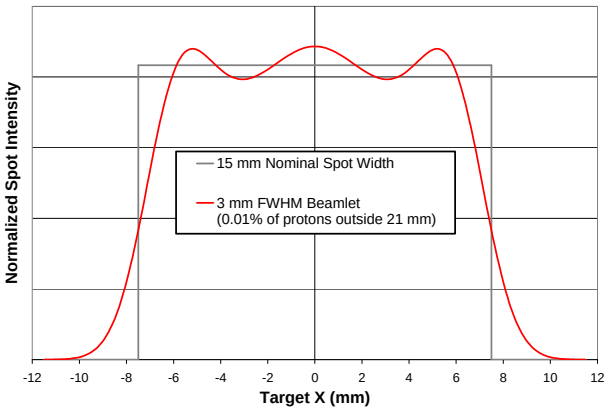

Fig. 4. Normalized Beam Spot Intensity.

A peak heat flux of 6 MW/m^2 is relatively high in water-cooled systems, therefore, it was important that the design had sufficient margin below the critical heat flux (CHF). Several correlations were used to predict CHF for the MTS system and the results are shown in Table 2.

Table 1. Target Cooling Water Inlet/Outlet Conditions

Velocity	10 m/s
Inlet Pressure	2.62 MPa
Inlet Temperature	40°C
Inlet Saturation Temperature	226°C
Inlet Subcooling Level	186°C
Outlet Pressure	2.07 MPa
Outlet Temperature	114°C
Outlet Saturation Temperature	214°C
Outlet Subcooling Level	101°C
Heat Transfer Coefficient	54,000 W/m^2°C
Outlet Wall Temperature	225°C

The majority of the correlations shown in Table 2 are for subcooled flow of water in uniformly heated, small-diameter, round tubes. The notable exception is Levy et al.[10] who studied CHF in small, rectangular channels. In their tests, there was heating right up to and in corners and edges, so their prediction is arguably too low for the more forgiving situation in MTS where the corners are not directly heated. Based on the predictions in Table 2, the MTS target design condition appears to be safely below CHF.

Table 2. CHF predictions under MTS conditions.

Investigator	**CHF (MW/m^2)**
Hall & Mudawar[4]	32.9
Modified Tong[5]	32.5
Gunther[6]	22.9
Sarma et al.[7]	20.2
Bowring[8]	18.7
Vandervort et al.[9]	17.5
Levy et al.[10]	3.7

The goal of the present study was to conduct a series of tests to verify the thermal-hydraulic predictions for the MTS water-cooled target. Of primary importance are single-phase heat transfer coefficient and pressure drop, which enable the determination of coolant pressure necessary to suppress boiling.

II. TEST FACILITY AND PROCEDURE

Figure 5 shows the flow loop that was constructed to supply light water to the test heater at the desired pressure, temperature, and flow rate. Water was pumped from a reservoir using two pumps in series: a 2-stage centrifugal pump followed by a variable-speed, high-pressure, multi-stage, centrifugal booster pump capable of exit pressures up to 4.1 MPa (600 psia). From the booster pump, water passed through a turbine flow meter on its way to the test section. The test section was mounted vertically with water flowing upward through the heated

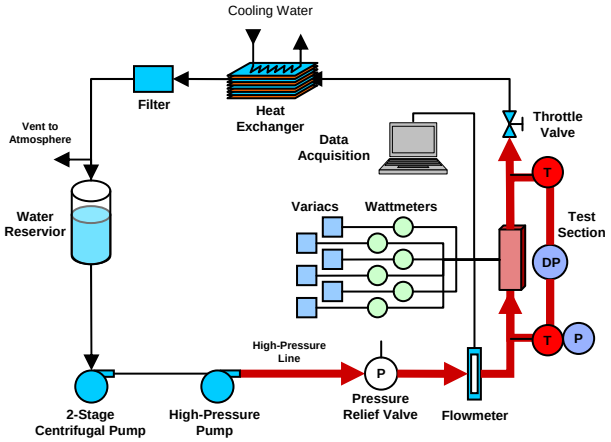

Fig. 5. Flow loop schematic.

section. Pressure was measured at the test section inlet and pressure drop was measured across the test section. Temperature was measured at the inlet and outlet of the test section with precision resistance temperature detectors (RTDs). A throttle valve downstream of the test section, combined with the variable-speed pump, enabled control of test pressure and flow rate. After the throttle valve, flow passed through a flat-plate heat exchanger and filter on its way back to the reservoir. The reservoir was vented to atmosphere.

The test section consisted of a 1 mm x 18 mm x 180 mm cooling channel machined from two blocks of oxygen-free copper as illustrated in Fig's 6, 7, and 8. This heater was based on the design by Qu and Mudawar[11] for generating high heat flux. The test section was machined in two identical halves that were then brazed together along the cooling channel midplane. Prior to brazing, the channel surface was sanded with 320 grit sandpaper to provide a surface of uniform consistency and known history. This surface is rougher than that planned for the MTS target plates.

Figure 7 shows the instrumentation of one of the copper block halves. To simulate high power delivered from the proton beam, the test section was fitted with 24 500-W cartridge heaters. The base of the heater block was tapered to a width of 1 cm (Fig. 7) and the channel wall thickness was set to 3 mm so that the temperature profile on the surface of the copper simulated that of a tungsten target plate. The temperature profile was determined by comparing a finite element analysis (FEA) simulation of the beam-heated tungsten target plate with that of the copper test heater.

Type-K thermocouples (4 per side) were located approximately 5 mm from the cooling channel surface (Fig's 7 and 8). Temperatures from these thermocouples were used, along with FEA, to determine the channel wall temperature, and thus, the average surface heat transfer coefficient. The test section was well insulated during the test.

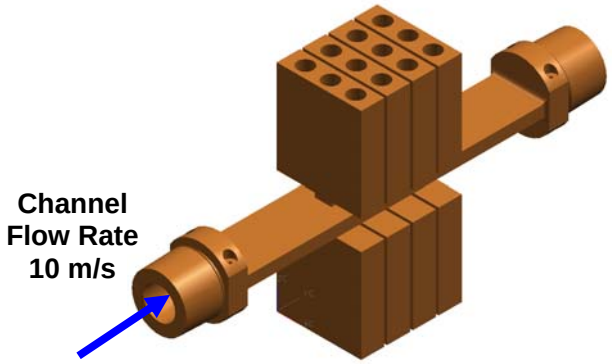

Fig. 6. Copper test section.

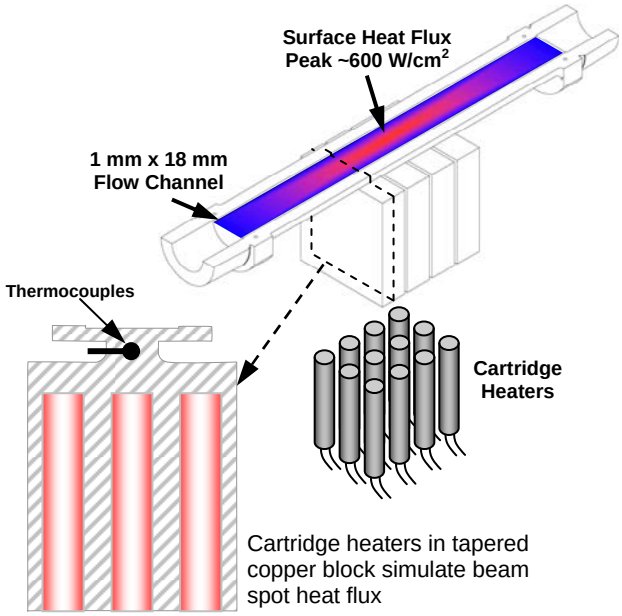

Fig. 7. Half of test section showing instrumentation.

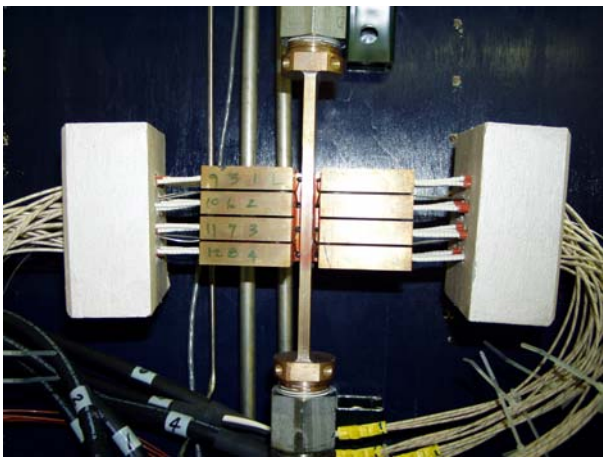

Fig. 8. Side view of instrumented, uninsulated test section mounted in flow loop.

During testing, the inlet conditions (flowrate, pressure, temperature) were set and then the desired power level was applied to the test heaters. Once steady-state conditions were achieved (usually about 10 minutes), data were taken and stored. Heat loss to the environment was calculated as the difference between the electric power input and the sensible energy gain in the water. Heat loss varied between 4 to 6% depending on the applied power. Experimental pressure drop measurements included additional plumbing losses upstream and downstream of the test section. These losses were calculated and subtracted from the experimental data to obtain the test section pressure drop. This experimental pressure drop was compared with the calculated test section pressure drop using a smooth-wall, turbulent Moody friction factor. Experimental uncertainties are shown in Table 3.

Table 3. Experimental Uncertainties

Parameter	**Uncertainty**
Water Temperature	+/-0.1°C
Heater Temperature	+/-1.0°C
AC Input Power @ Full Power	+/-10.6 W
Inlet Pressure (% of reading)	0.3%
Pressure Drop	2.2 kPa

The test data were subsequently used as input for a 3D, ¼-symmetry, FEA model of the test heater (Fig. 9). Uniform heat flux was applied to the cylindrical walls to represent the cartridge heater inputs. The input power used was the recorded electrical power minus the calculated heat loss. For the convection boundary condition, the experimental coolant temperature was applied to the wall in 10 increments linearly increasing from inlet to outlet.

The heat transfer coefficient used for the FEA convection boundary condition was calculated from the test data using the following correlation of Sieder and Tate[3]

$$Nu_D = 0.027 Re_D^{4/5} Pr^{1/3} \left(\frac{\mu}{\mu_s} \right)^{0.14} \quad (1)$$

where Nu_D and Re_D are the Nusselt and Reynolds numbers, respectively, with characteristic length of hydraulic diameter based on heated perimeter, Pr is the Prandtl number, and μ is the dynamic viscosity. All properties in Eq. (1) were evaluated at the average of the bulk fluid and wall temperatures except for μ_s, which was evaluated at the average wall temperature. The wall temperatures used for the property evaluation in Eq. (1) were obtained iteratively from the resulting heat transfer coefficient.

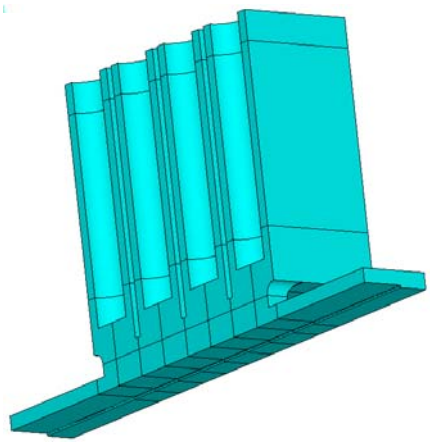

Fig. 9. ¼-Symmetry FEA model of the test heater.

Temperature-dependent thermal conductivities used for the copper in the FEA simulation were the recommended values from the Purdue Thermophysical Properties of Matter Database[12]. These data are for well-annealed, high-purity copper and are considered accurate to within +/-2% of the true values near room temperature and +/-4% at high temperatures.

III. RESULTS AND DISCUSSION

Test data were acquired for input heat fluxes ranging from 1 to 6.5 MW/m^2, inlet pressures from 0.2 to 3 MPa, inlet temperatures from 25 to 90°C, and inlet velocities from 6.5 to 12 m/s. Figures 10, 11, and 12 show a combination of experimental and FEA results for a typical high-heat-flux (6.07 MW/m^2) single-phase flow condition. For these figures, the inlet velocity is 10 m/s and the inlet pressure and temperature are 541 kPa and 31.9°C, respectively.

Figure 10 shows the FEA temperature contours in the copper test heater. This figure illustrates that at high heat flux conditions, peak temperatures within the copper block easily exceed 600°C. These FEA results were used to extract the temperatures within the copper block at the eight thermocouple locations.

A comparison of these FEA and experimental copper block temperatures are shown in Fig. 11. The thermocouples are numbered 1 through 4 from inlet to outlet. Data are shown for thermocouples on the right-hand side (RHS) and left-hand side (LHS), as defined by the view in Fig. 8. The RHS temperatures are slightly higher than the LHS temperatures. This is because the holes drilled in the block for the RHS thermocouples are slightly further from the channel surface (by approximately 0.4 mm) than those for the LHS. The FEA temperature results were interrogated at the as-tested thermocouple locations to extract the simulation data for comparison in Fig. 11.

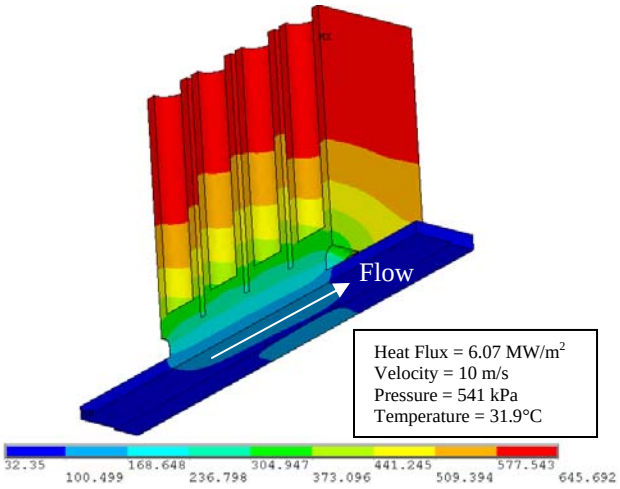

Fig. 10. FEA temperature contours (°C).

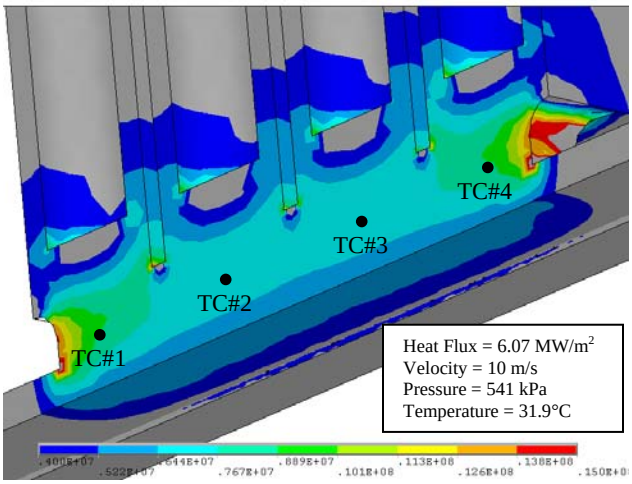

Fig. 12. FEA heat flux contours (W/m^2).

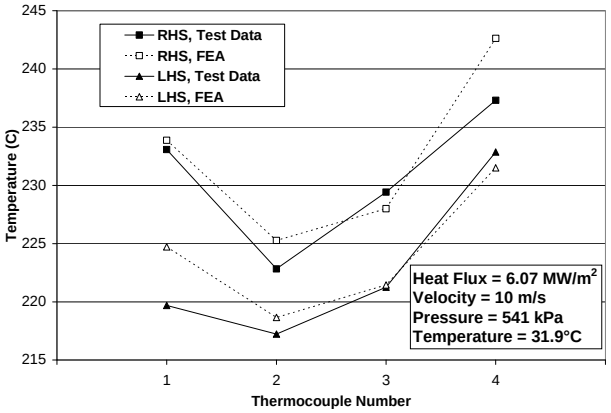

Fig. 11. Comparison between experimental and FEA test section temperatures.

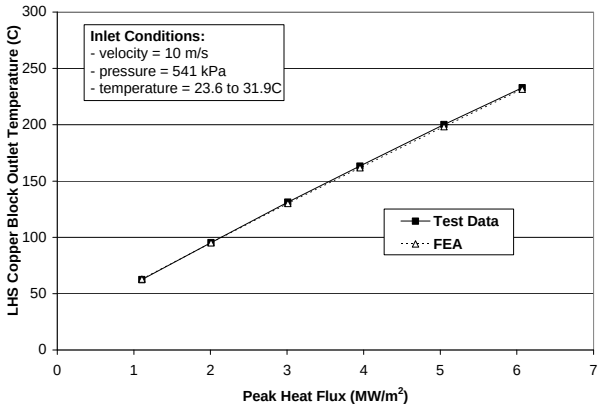

Fig. 13. Experimental temperature comparison with FEA as a function of surface heat flux.

The temperature initially decreases from location 1 to 2, and then increases toward the outlet. The temperatures at locations 1 and 4 are elevated slightly above a logical linearly increasing trend from inlet to outlet due to the tapering of the copper heater block near those locations. This tapering results in a higher heat flux through those locations as illustrated in Fig. 12.

Figure 12 shows heat flux contour results from the FEA simulation. This plot clearly shows the non-uniform heat flux on the channel wall. The surface heat flux ranges from a peak of 6 MW/m^2 at the center of the channel to approximately 4 MW/m^2 near the corners. This non-uniform heat flux distribution simulates that of the beam-heated tungsten target plates.

Figure 13 shows a comparison between the experimental data and FEA results for the temperature at location 4 on the LHS as a function of surface heat flux. The experimental vs. FEA temperature comparisons in Fig's 11 and 13 are quite good. As mentioned previously, the only non-experimental boundary condition applied to the FEA model was the heat transfer coefficient, which was calculated using the correlation in Eq. (1). This favorable comparison indicates that Eq. (1) can be used with confidence to compute single-phase heat transfer coefficients for the MTS target.

Figure 14 illustrates the onset of nucleate boiling in the test heater. This figure shows experimental copper block outlet temperature vs. inlet pressure for varying test section velocities. Velocities range from 6.5 to 9 m/s. Subcooling levels are shown in the legend. The data are for a heat flux of 6.5 MW/m^2 and an inlet temperature of 41°C. The data were obtained by setting a desired velocity and then lowering the pressure as far as the experimental facility would allow. As the pressure is lowered at 6.5 and 7.5 m/s, the outlet temperature eventually experiences a sharp decline, indicating that subcooled nucleate boiling is occurring and the heat transfer coefficient is increasing. At 9 m/s, however, the pressure could not be lowered far enough to trigger the onset of nucleate boiling. The results in Fig. 14 indicate that the MTS design operating condition of 6 MW/m^2, 10 m/s, and 2.62 MPa provides ample margin above the onset of nucleate boiling.

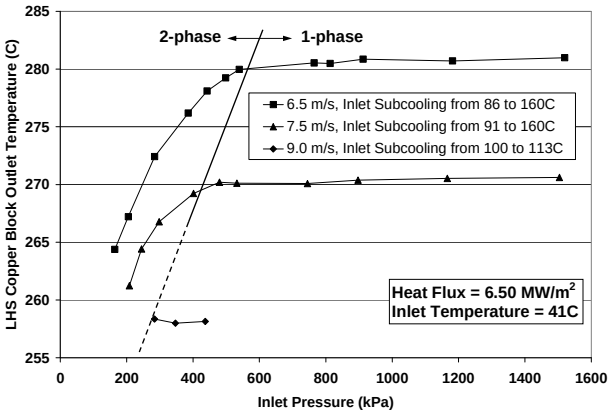

Fig. 14. Onset of subcooled nucleate boiling at test section exit.

In order to explore the possibility of CHF occurring in the target, two transient tests were performed at a heat flux of 6.5 MW/m^2. The facility cooling water was turned off and the test section inlet temperature was allowed to climb as high as 90°C. Figure 15 shows the results of these tests at velocities of 8.6 and 10 m/s. The duration of each test was approximately 20 minutes. Even though inlet pressures were an order of magnitude below MTS design pressure, CHF did not occur. The final inlet subcooling level for each test was approximately 55°C.

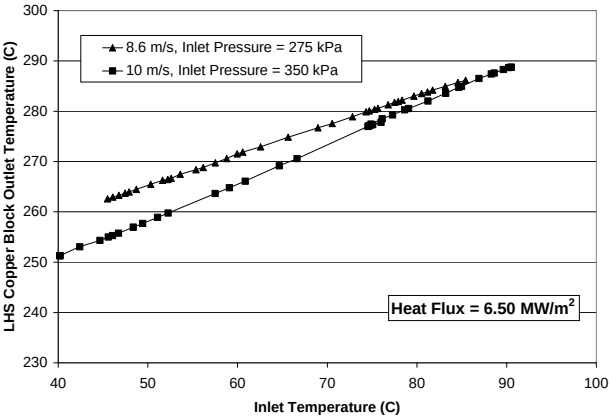

Fig. 15. Transient exploration of CHF.

Single-phase, test section pressure drop data were obtained by subtracting estimates for upstream and downstream plumbing losses (tees, expansions, contractions, etc). These pressure drop data were within 10% of the calculated test section pressure drop using a smooth-wall, turbulent Moody friction factor.

IV. CONCLUSIONS

Tests were performed on a high-heat-flux test section to simulate thermal-hydraulic conditions of the water-cooled, MTS target. Results from these tests and subsequent FEA heater simulations indicate that a) a simple, single-phase handbook correlation can be used with confidence to predict MTS target heat transfer coefficients, and b) the MTS design provides adequate margin above the onset of nucleate boiling and below the CHF.

ACKNOWLEDGMENTS

This work is sponsored by the U.S. Dept. of Energy.

REFERENCES

1. T.A. Broome, J. Chiba, S. Sawada, H. Miyatake and M. Furusaka, "The Design of the ISIS Target," *Proc. Int. Workshop JHF Sci. (JHF98)*. Vol. 3, p.41 (1998).
2. M. Kawai, K. Kikuchi, H. Kurishita, J.F. Li and M. Furusaka, "Fabrication of a Tantalum-Clad Tungsten Target for KENS," *J. Nuc. Mat.*, **296**, 312 (2001).
3. E.N. Sieder and G.E. Tate, "Heat Transfer and Pressure Drop of Liquid in Tubes," *Ind. Eng. Chem.*, **28**, 1429 (1936).
4. D.D. Hall and I. Mudawar, "Critical Heat Flux (CHF) for Water Flow In Tubes–II. Subcooled CHF Correlations," *Int. J. Heat Mass Trans.*, **43**, 2605 (2000).
5. G.P. Celata, M. Cumo and A. Mariani, "Assessment of Correlations and Models for the Prediction of CHF In Water Subcooled Flow Boiling," *Int. J. Heat Mass Trans.*, **37**, 237 (1994).
6. F.C. Gunther, "Photographic Study of Surface Boiling Heat Transfer to Water with Forced Convection", *Trans. ASME*, **73**, 115 (1951).
7. P.K. Sarma, V. Srinivas, K.V. Sharma, V. Dharma Rao and G.P. Celata, "A Correlation to Evaluate Critical Heat Flux In Small Diameter Tubes Under Subcooled Conditions of the Coolant," *Int. J. Heat Mass Trans.*, **49**, 42 (2006).
8. R.W. Bowring, "A Simple But Accurate Round Tube, Uniform Heat Flux, Dryout Correlation Over the Pressure Range 0.7 to 17 MN/m^2 (100-2500 psia)," AEEW-R-789, Atomic Energy Research Establishment, Winfrith (1972).
9. C.L. Vandervort, A.E. Bergles and M.K. Jensen, "An Experimental Study of Critical Heat Flux In Very High Heat Flux Subcooled Boiling", *Int. J. Heat Mass Trans.*, **37**, Suppl. 1, 164 (1994).
10. S. Levy, R.A. Fuller and R.O. Niemi, "Heat Transfer to Water In Thin Rectangular Channels", *J. Heat Trans.*, **81**, 129 (1959).
11. W. Qu and I. Mudawar, "Thermal Design Methodology for High-Heat-Flux Single-Phase and Two-Phase Micro-Channel Heat Sinks," *IEEE Trans. Comp. Pack. Tech.*, **26**, 598 (2003).
12. Purdue Thermophysical Properties of Matter Database, www.cindasdata.com.